Advanced Composite Materials
Publication details, including instructions for authors and subscription information:
http://www.tandfonline.com/loi/tacm20

Compressive property degradation of composite stiffened panel due to debonding and delaminations

Hiroshi Suemasu , Keisuke Kurihara , Keiji Arai , Osamu Majima & Takashi Ishikawa

Version of record first published: 02 Apr 2012.

To cite this article: Hiroshi Suemasu , Keisuke Kurihara , Keiji Arai , Osamu Majima & Takashi Ishikawa (2006): Compressive property degradation of composite stiffened panel due to debonding and delaminations, Advanced Composite Materials, 15:2, 139-151

To link to this article: http://dx.doi.org/10.1163/156855106777873897

Adv. Composite Mater., Vol. 15, No. 2, pp. 139–151 (2006)

Compressive property degradation of composite stiffened panel due to debonding and delaminations*

HIROSHI SUEMASU [1,†], KEISUKE KURIHARA [2], KEIJI ARAI [3], OSAMU MAJIMA [1] and TAKASHI ISHIKAWA [4]

[1] *Department of Mechanical Engineering, Faculty of Science and Technology, Sophia University, Tokyo, Japan*
[2] *Graduate School, Sophia University, Tokyo, Japan*
[3] *Mitsubishi Heavy Industry, Nagoya, Japan*
[4] *Japan Aerospace Exploration Agency, Chofu, Tokyo, Japan*

Received 25 January 2005; accepted 30 May 2005

Abstract—The effect of localized damage due to impact on compressive buckling as well as postbuckling behaviors of blade stiffened composite plates was numerically studied. A partial debonding between a skin panel and a flange and multiple delaminations in the skin panel were chosen as the localized damage. The three-dimensional composite elements used to analyze the compressive behavior of the stiffened panel with multiple delaminations was found to be suitable for this kind of complex composite structure. The contact problem between the skin and flange panels was approximated by a spring element with no restraint of the positive relative displacement and a strong restraint of the negative displacement. At the delaminations in the skin panel, which tended to close during compression, the normal relative displacement was constrained to prevent the delaminated portions from overlapping; this constraint made the convergence of the solution quite smooth compared to the case where the contact problem was exactly considered. When a debonded area only was located at the edge of the flange, no notable reduction of compressive buckling load was found until the size of the debonding reached a half wavelength of the buckling mode. The compressive buckling load dropped significantly when multiple delaminations, which were small in comparison to the half wavelength of the buckling mode, accompanied the skin-flange debonding. The energy release rate distributions at the damage edges, calculated using the virtual crack closure technique, increased quite rapidly, particularly in the transverse direction after buckling became sufficient to increase the delamination.

Keywords: Composite stiffened panel; debonding; buckling; energy release rate.

*Edited by the JSCM.

†To whom correspondence should be addressed. E-mail: Suemasu@sophia.ac.jp

1. INTRODUCTION

Composite laminates are being applied to the stiffened panels in aerospace structures because of their high specific strength and stiffness. However, many issues must be overcome in order to use composite materials more efficiently. One issue is the effect of localized damage, such as impact damage, on the overall strength. It is quite difficult to assess the effect of damage on the final failure strength of stiffened composite panels because of their complex configuration consisting of inhomogeneous materials with many interfaces and because of their complicated deformation history during loading. Both elaborate experiments and numerical research must be conducted to study the compressive performance of the composite stiffened panels.

A stiffened panel of composite material using a high toughness and high thermal resistant resin as its matrix (CF/PIXA) has been developed by the joint efforts of the Japan Aerospace Exploration Agency, Fuji Heavy Industry Co. and Mitsui Chemical Company [1]. A series of compression tests were conducted on the stiffened panels with and without impact damage at the flange portion. Because of the high interlaminar toughness of these panels, the impact damage showed little effect on their rupture strength, even when there was significant damage. This result indicates that the material system has a high tolerance to local impact damage. However, the experiment alone could neither show the margin to failure of the material with damage nor the relationship between the damage and the reduction of the strength of the stiffened panel.

The compressive behavior of composite stiffened panels is not only an interesting topic in mechanical engineering but also an important issue in the aerospace structural design. A numbers of studies have been performed to investigate the various problems [2–7]. The effect of damage on the compressive behavior of stiffened panels has been studied by several researchers. Ishikawa *et al.* carried out a careful experimental study on the compressive problem of stiffened panels with impact damage and showed interesting results [1, 8]. Suemasu *et al.* studied the effects of edge delamination on the stiffener portion through Rayleigh-Ritz approximation and experiment [9, 10]. Raju *et al.* discussed the stability of the delamination crack at the end portion of the stiffener [11]. Wang *et al.* calculated the energy release rate of the delamination between the flange and skin panel by using both a three-dimensional element and shell elements and showed that both results correlate with each other [12]. Park *et al.* calculated the energy released rate of a panel with a partially debonded stiffener [13]. Suemasu *et al.* numerically studied the buckling and postbuckling behavior of through debonding [14] and partial debonding [15] at the flange and skin-panel interface and showed that an obvious reduction of the buckling load did not occur until the size of the debonding reached the dimension of the half wave of the first buckling mode.

In the present paper we will discuss the effects of the debonding between the stiffener and skin panel as well as the multiple delaminations in the skin panel on compressive behavior.

2. NUMERICAL MODEL OF THE DAMAGED STIFFENED PANEL AND FINITE ELEMENT ANALYSIS

We considered a blade-stiffened panel [1] made of carbon fiber and a high toughness and high thermal resistant resin (PIXA) as shown in Fig. 1. The mechanical properties of the individual lamina are $E_L = 152.4$ GPa, $E_T = 8.06$ GPa, $\nu_{LT} = 0.344$, $G_{LT} = 4.69$ GPa and $G_{TT} = 2.62$ GPa. The dimensions of the panel are also shown in Fig. 1. The stacking sequences of the portions are listed in Table 1, where the 0° direction is horizontal (x-axis) and transverse to the load as shown in Fig. 1. The boundary conditions are

$$
\begin{array}{lllll}
w = 0, & w,_y = 0, & \tau_{xy} = 0, & v = v_0, & \text{at the upper edge,} \\
w = 0, & w,_y = 0, & \tau_{xy} = 0, & v = 0, & \text{at the lower edge,} \\
w = 0, & M_x = 0, & \tau_{xy} = \sigma_x = 0, & & \text{at the side edges.}
\end{array} \tag{1}
$$

The frictional force was assumed to be zero at all edges to minimize the local distortional effect of the boundary. The horizontal displacement was constrained at the lower left end to make the problem statically determinate. The stiffener portions were fabricated as shown in the Fig. 1b. The damage illustrated in Fig. 1 was located at the center of the right flange and the size was characterized by the length of the parallel portion l_d and the radius r_d.

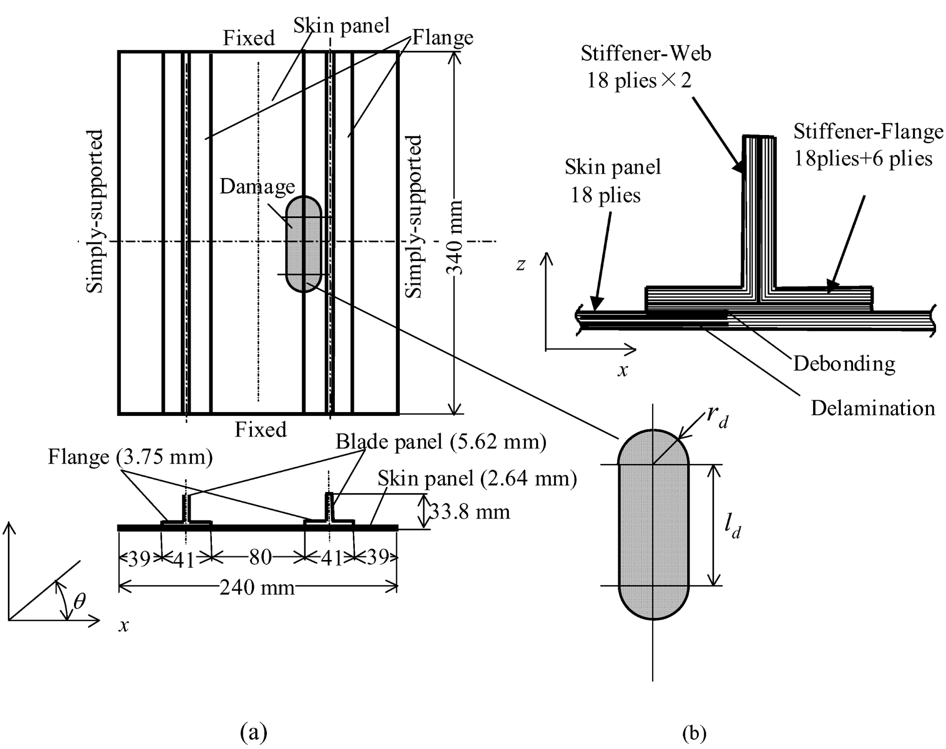

Figure 1. Dimensions and coordinate system of stiffened panel.

Table 1.
Stacking sequences of each portion

	Ply number	Stacking sequence
Skin panel	18	$[45/90/-45/0/0/45/90/-45/0]_{\mathrm{sym}}$
Stiffener-flange	24	$[45/0/-45/90/45/0/0/-45/0/0/-45/0/0/45/90/-45/0/45$ $/45/0/-45/-45/0/45]$
Stiffener-web	36	$[45/0/-45/90/45/0/0/-45/0/0/45/0/0/45/90/-45/0/45]_{\mathrm{sym}}$

Table 2.
The intact and damaged models calculated

Model name	Number of delaminations	l_f (mm)	r_f (mm)	Element number	Node number
Model 0	—	0	—	2920	17 836
Model 1-0	0	0	11	2652	14 706
Model 1-1	1	0	11	2652	15 830
Model 1-2	2	0	11	3492	20 461
Model 1-3	3	0	11	4332	25 095
Model 2-0	0	36	11	3348	18 469
Model 3-0	0	60	11	2568	15 807

We used a commercially available finite element code (ABAQUS 6.3 Standard [16]). In order to discretize the stiffened panels of the laminated composites with the multiple delaminations, we used three-dimensional 20-node isoparametric brick elements specially programmed for composite laminated structures. A spring element was placed in the debonded portion between the skin and the flange; the spring element had no constraint in the tensile direction and a strong spring constant in the compression direction. Although the debonded portion tended to open in most case, the constraint might not be necessary if the initial opening of the debonded portion is set appropriately. Since all the delaminated portions in the skin panel tended to close during compression, the relative displacement in the thickness direction was constrained. Because the stacking sequence of the flange portion was asymmetric, no initial imperfection was needed to be implied. The cases we calculated are listed in Table 2. The delamination is placed at the mid-plane of the skin panel for the model 1-1, at the 6th and 12th interfaces from the surface for the model 1-2 and at fourth, center (ninth) and 14th interfaces for the model 1-3, respectively. Figure 2 shows three finite element meshes for undamaged (model 0) and damaged plates.

3. NUMERICAL RESULTS AND DISCUSSIONS

The convergence behavior of the buckling load with the discretization by the composite brick element was studied here by dividing the skin panel in the thickness

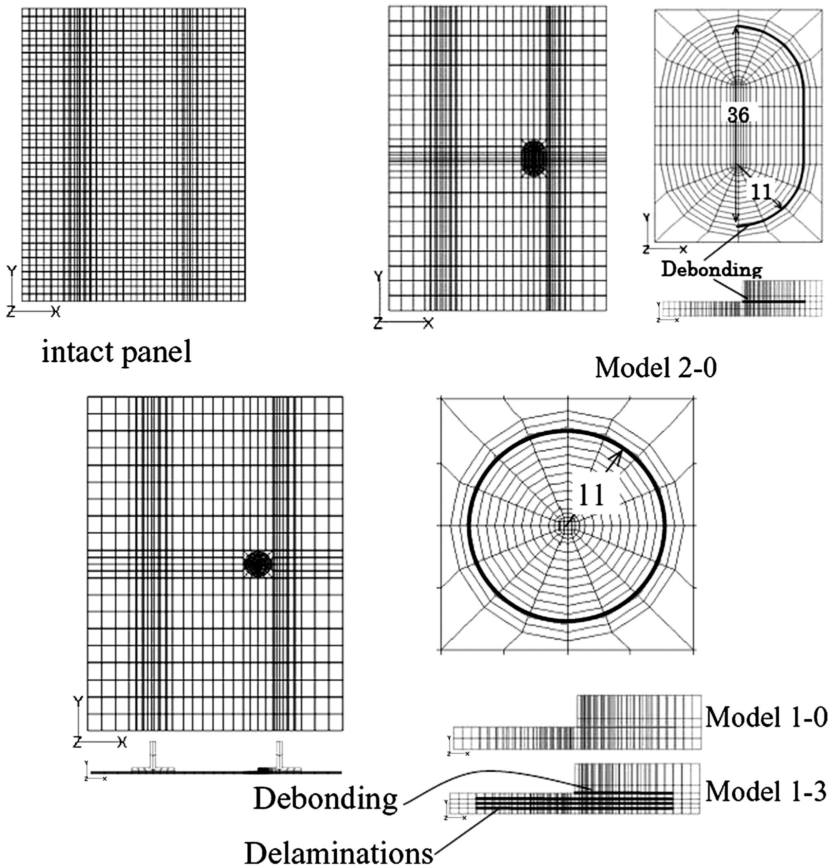

Figure 2. Finite element models of intact and damaged panels.

direction and the results are listed in Table 3. The discretization in the in-plane direction used in the present analysis was determined to be sufficient because little improvement was obtained after further refinement of the elements in the in-plane direction. Because the skin panel is an 18 ply laminate, the solution of the 18 division model is thought to be a well-converged solution. The result showed that the solution from the model with only one layer of elements in the thickness direction was 1.9% higher than the solution of 18 layers and the solution with two layers was 1.4% higher. The 20 node composite brick elements which can express only the displacement of 2nd order polynomial cannot simulate very well the displacement field of laminate, which has almost a piece-wise linear variation in the thickness direction. This limitation of the composite brick element is similar to that of shell elements based on classical or Mindlin-type plate theory. Global phenomena such as the buckling mode and relative values of each buckling loads were obtained by the 1-layer model and were quite similar to that obtained by the 18-layer model. The buckling modes of the intact stiffened plate are shown in Fig. 3. The first buckling mode had five half-waves in the loading direction, while the

Table 3.
Number of divided layers of the skin panel in the thickness direction and buckling load of intact stiffened plate (kN)

Number of layers	1	2	3	4	6	18
1st mode	300.12	298.11	296.81	296.60	295.38	294.70
2nd mode	301.45	299.48	298.11	297.95	296.69	296.03
3rd mode	328.92	327.58	325.48	324.86	323.68	322.89

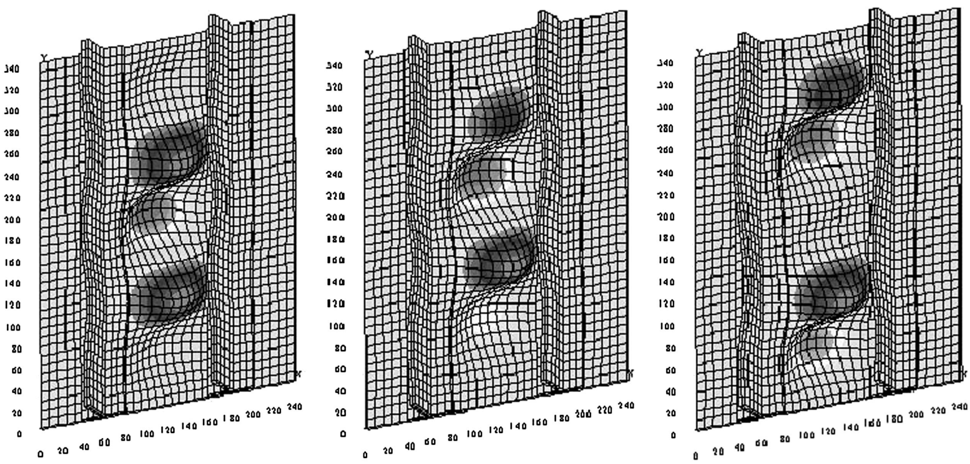

(a) 1-st (302kN) (b) 2-nd (303kN) (3) 3-rd (331kN)

Figure 3. Buckling modes of intact stiffened panel.

second buckling mode had four half-waves. The first and second buckling loads were very similar to each other. The numerical results explained satisfactory the experimental results obtained by Ishikawa *et al.* [1], where the average buckling load was about 290 kN and the buckling modes observed in the plate with uniform skin thickness and slightly tapered skin were 5-wave pattern and 4-wave pattern, respectively. Considering the efficiency of the calculation we basically adopted two layer models for convenience when further subdivision was not necessary to model the damaged portion.

The buckling loads of the damaged plates were obtained from the nonlinear analysis using the δ^2-method and the values listed in Table 4. The buckling loads of the model with only a debonding between the flange and skin panel decreased with the debonding size. However, the reduction of the buckling load was not significant: less than 10% even for model 3-0, which had a very large debonding area. The effect of the delaminations accompanying the debonding on the buckling behavior was studied by increasing the number of delaminations. The buckling loads of models 1-1 and 1-2 were slightly smaller than that of model 1-0, while the buckling load of model 1-3 with three multiple delaminations was quite low (a 30% reduction).

Table 4.
Buckling loads of intact and damaged stiffened panels obtained from nonlinear analysis

Model	Buckling load (kN)
Intact panel	298
Model 1-0	293
Model 1-1	292
Model 1-2	290
Model 1-3	217
Model 2-0	286
Model 3-0	281

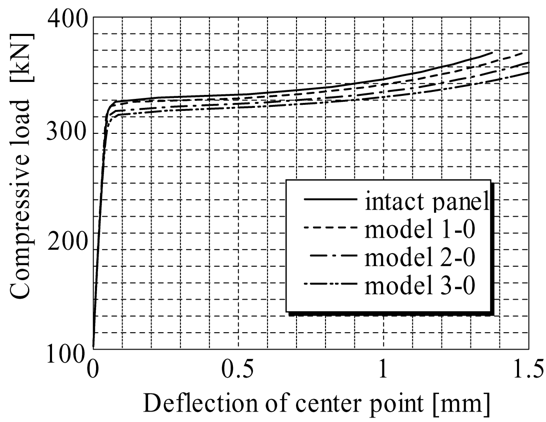

Figure 4. Relationships between the load and the center deflection for the panels only with a debonding.

Multiple delaminations are thought to be an important factor for the reduction of compressive strength of the composite stiffened panel due to impact damage.

The applied compressive loads are plotted against the deflection of the center of the skin panels for the panel with only a debonding (Fig. 4) and those with both a debonding and delaminations (Fig. 5). The deflection of the center of the circular delaminated portion of model 1-3 is also plotted in Fig. 5 to highlight the local buckling behavior of the damaged portion. The reduction of the resisting force due only to a debonding was insignificant considering the size of the area, while the reduction of the buckling load was significant when multiple delaminations accompanied the debonding. Figures 6–8 show the deformations of the intact and damaged panels during compression. A uniform small deflection increased with the load at the start of the loading for all cases due to the asymmetric stacking sequence. When the applied load approached the buckling load, the deformation which was similar to the first buckling mode increased rapidly and the deformation grew with the increase in load. Model 1-0, which had a small semicircular debonding, showed little difference in the compressive behavior from that of the intact panel, as expected from the buckling analysis. For model 2-0, the deformation at the center

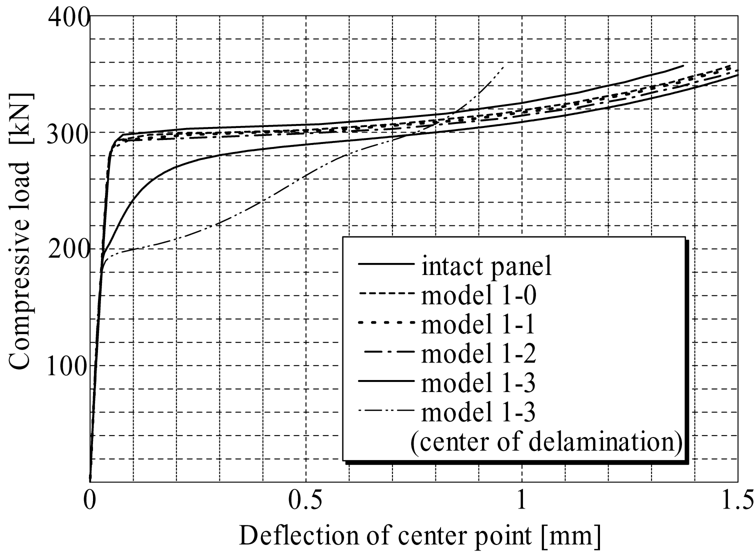

Figure 5. Relationships between the load and the center deflection for the panels with a debonding and multiple delaminations.

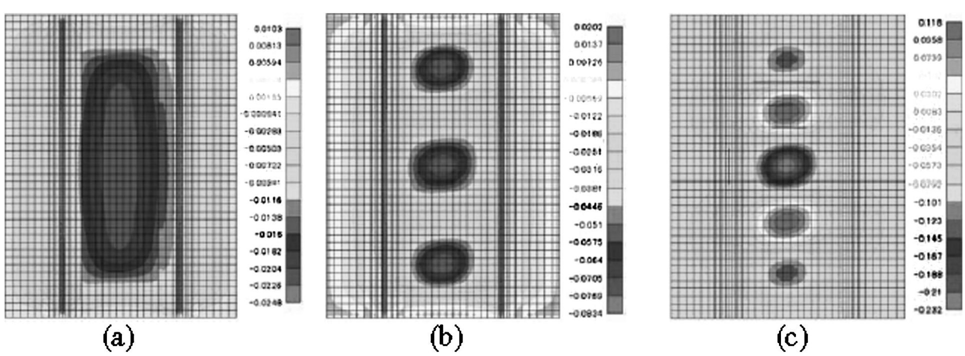

Figure 6. Deformed shapes of the intact panel during compression, (a) 148 kN, (b) 298 kN, (c) 303 kN.

portion became large compared to the deformation at the other portions (Fig. 7): this is thought to be a major reason for the decrease of the buckling load. Models 1-1 and 1-2, whose results are not shown in the paper, had behaviors similar to that of the intact panel (Fig. 6), while model 1-3 with three delaminations showed different behaviors from the other models. As shown in Fig. 8, only the delaminated portion deformed when the load approached the local buckling load ($\approx$200 kN). The global deformation gradually increased as the load increased. The deformed shape of the delaminated portion inclined slightly because the bending stiffness was not isotropic. It shows that the local buckling strains of the delaminated portions of the models 1-1 and 1-2 are higher than the buckling strain of the stiffened panel without

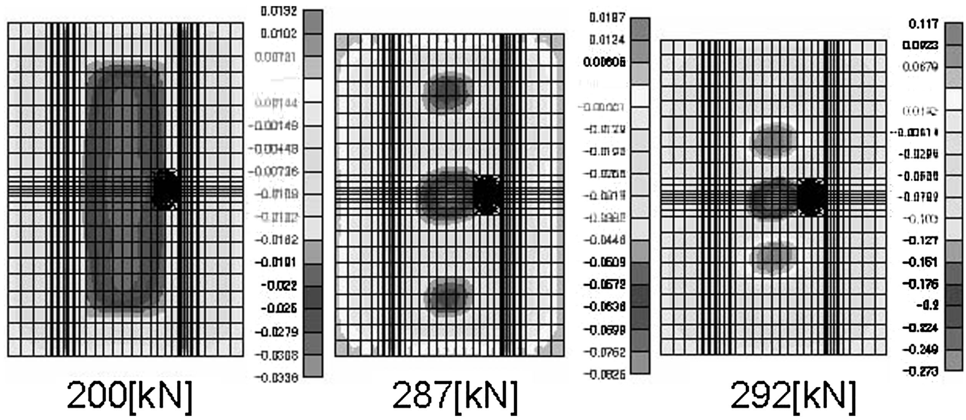

Figure 7. Deformed shapes of the damaged panel model 2-0.

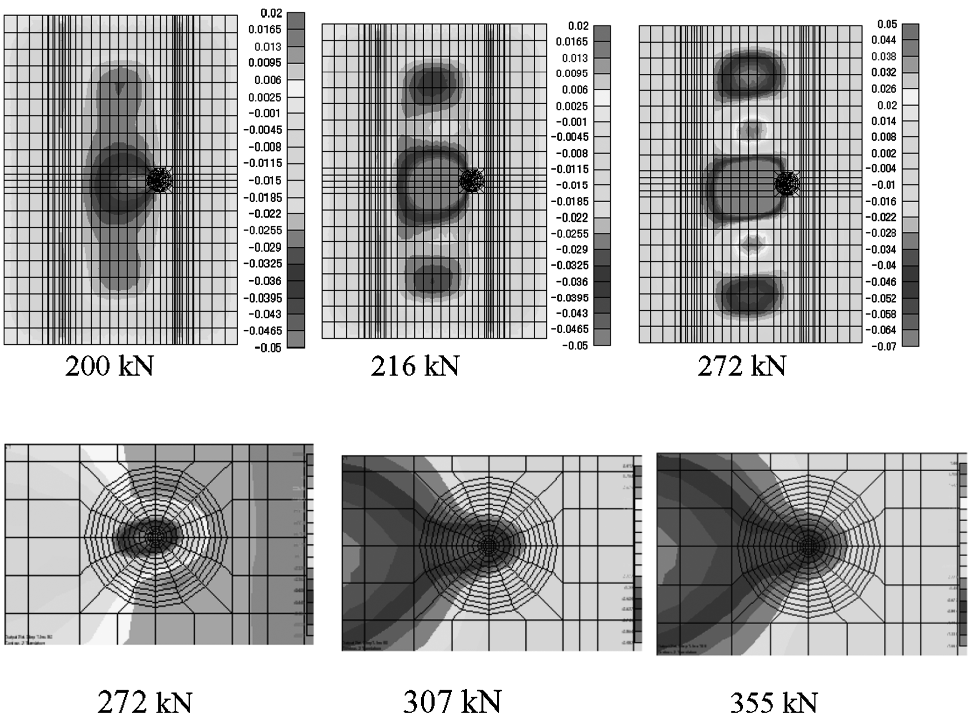

Figure 8. Deformed shapes of the damaged panel model 1-3.

damage, while that of the model 1-3 is lower than the buckling strain of the intact stiffened panel.

The energy release rate distribution is calculated to discuss the stability of the damage. The critical mode I energy release rate of the CF/PIXA is 1.4 kJ/m^2, which is much higher than that of tough epoxy matrix composite (T800H/3900-2) of 0.32 kJ/m^2. The energy release rate distribution for the model 2-0 is plotted in

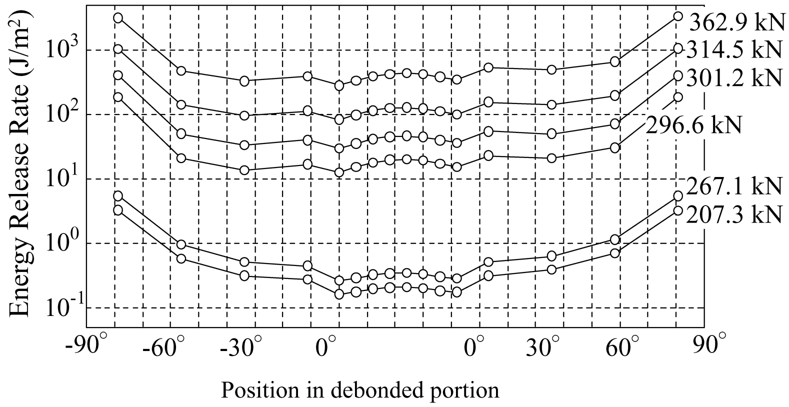

Figure 9. Energy release rate distribution around the debonding between skin panel and flange portion for model 2-0.

Fig. 9. The energy release rate did not increase enough for the debonded area to propagate further (except the two ends where the stress singularity was expected) until the load became much higher than the buckling load. The energy release rate distributions along the debonding and delamination fronts for the model 1-3 are plotted in Figs 10–12. The energy release rate increased rapidly when the load exceeded the low local buckling load. The energy release rate was particularly large in both transverse directions of the debonded and delaminated portions. The shape of the energy release rate distribution changed slightly when the global deformation became large compared to that of the center of the delamination. The value of the energy release rate in the 180 degree direction reached a maximum as the local buckling region became a local minimum as shown in Figs 10 and 11. The distribution shapes of the energy release rate are compared in Fig. 12 for the local buckling region and the globally deformed regions. The maximum values and the distribution shapes of energy release rates at all the delaminations did not differ much from each other. The energy release rates at the delaminations in the skin panel were slightly smaller than the interface between the flange and skin panel. The energy release rate was slightly larger in the flange side ($|\theta| < 90°$) than in the other side ($|\theta| > 90°$).

4. CONCLUSIONS

We have numerically studied the compressive property degradation of composite stiffened panels by using composite brick elements prepared by a commercially available finite element package. The effect of the discretization in the thickness direction on the accuracy of the solution was similar to the case of the shell element. It was found to be convenient to model three-dimensionally complex structures made of composite laminates. From the numerical analysis of the compressive behavior of the stiffened panels with damage we have some mechanism of the

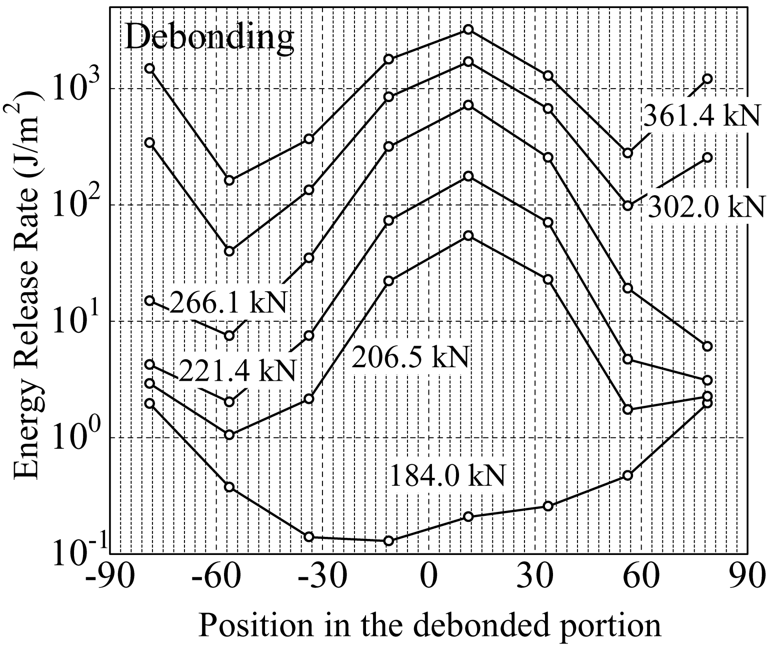

Figure 10. Energy release rate distribution around the debonding between skin panel and flange portion for model 1-3.

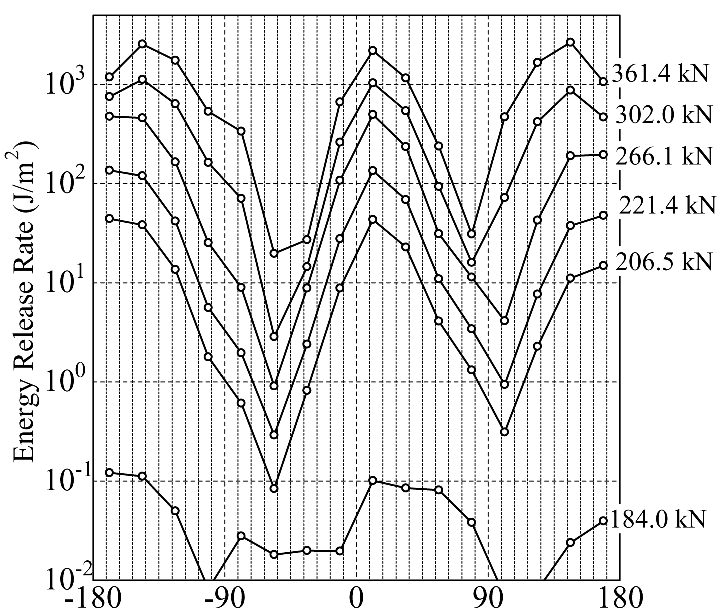

Figure 11. Energy release rate distribution around the center delamination for model 1-3.

reduction of the compressive strength due to the damage. When only a debonding occurred at the flange and skin–panel interface, which is the most damage-prone portion of the panel, the reduction of the strength was not noticeable until the debonding size was considerably large. When multiple delaminations accompanied the debonding, reduction of the buckling load became noteworthy. The energy release rate grew rapidly with the increase of local buckling deformation. The reduction of the compressive strength of the stiffened panels due to impact damage is caused by a similar mechanism of the CAI strength reduction of the plates specified by SACMA or NASA standard. From the above findings we may say that the tough interface is quite effective to improve the strength of the impact damaged stiffened plate for two reasons. The first is that the size of the damage with respect to the impact energy may be reduced, as stated in other research. The other is that the load of damage instability, which was thought to be related to the ultimate strength of the stiffened panel, increases with the interlaminar toughness when the damage size is identical.

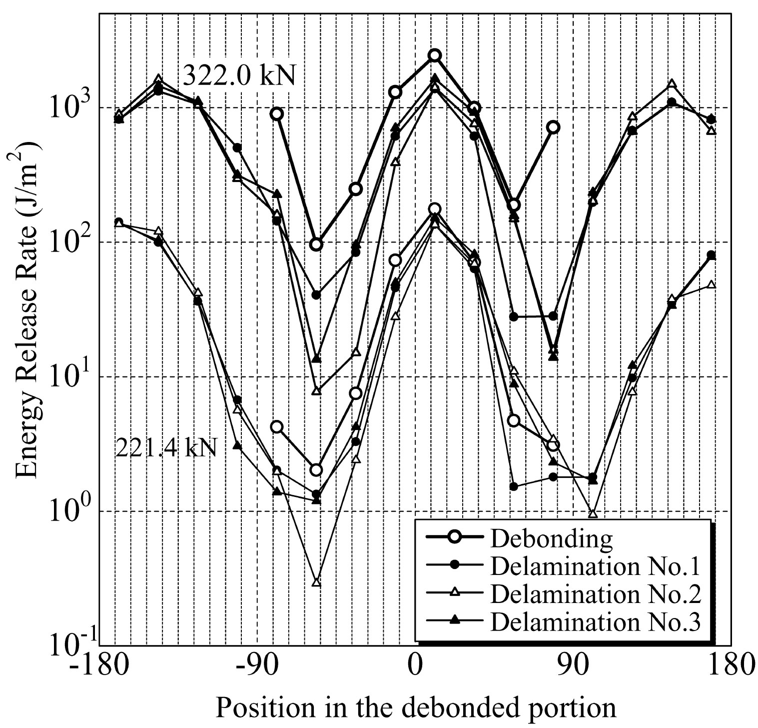

Figure 12. Comparison of the energy release rate distributions of the damage edges at the local buckling region and globally deformed region for model 1-3.

REFERENCES

1. T. Ishikawa, M. Matsushima, E. K. G. Lim, Y. Hayashi and M. L. Scott, Compression after impact (CAI) behavior of CF/PIXA stiffened panels for HSCT empennage, in: *Proc. 13th Ann. Tech. Conf. Compos. Mater.*, Baltimore, Maryland, USA, pp. 1776–1786 (1998).
2. J. H. Starnes, N. F. Knight, Jr. and M. Rouse, Postbuckling behavior of selected flat stiffened graphite-epoxy panels loaded in compression, *AIAA Journal* **23**, 1236–1246 (1985).
3. N. F. Knight, Jr. and J. H. Starnes, Jr., Postbuckling behavior of selected curved stiffened graphite-epoxy panels loaded in axial compression, *AIAA Journal* **26**, 344–352 (1988).
4. M. W. Hyer and D. Cohen, Calculation of stresses in stiffened composite panels, *AIAA Journal* **26**, 852–857 (1988).
5. H. Alesi, V. M. Nguyen, N. Mileshkin and R. Jones, Global/local postbuckling failure analysis of composite stringer/skin panels, *AIAA Journal* **36**, 1699–1705 (1998).
6. C.-W. Kong, I.-C. Lee, C.-G. Kim and C. S. Hong, Postbuckling and failure of stiffened composite panels under axial compression, *Compos. Sci. Technol.* **42**, 13–21 (1998).
7. B. G. Falzon, K. A. Steven, M. Goia and G. A. O. Davies, Postbuckling failure of a blade stiffened carbon-epoxy compression panel, in: *Proc. 13th Ann. Tech. Conf. Compos. Mater*., Baltimore, Maryland, USA (1998).
8. T. Ishikawa, K. Hayashi and T. Matsushima, Compression after impact strength of stiffened panels made of CF/PEEK and CF/epoxy, *J. Japan Soc. Aeronaut. Space Sci.* **44**, 319–328 (1994).
9. H. Suemasu, K. Gozu, K. Hayashi and T. Ishikawa, Compressive buckling of rectangular composite plates with a free-edge delamination, *AIAA Journal* **33**, 312–319 (1995).
10. H. Suemasu, M. Kawauchi, K. Gozu, K. Hayashi and T. Ishikawa, Effects of a free edge delamination on buckling of rectangular composite plates with two fixed loading and one simply-supported side edges, *Adv. Composite Mater.* **5**, 185–200 (1996).
11. I. S. Raju, R. Sistla and T. Krishnamurthy, Fracture mechanics analysis for skin-stiffener, *Engng. Fract. Mech*. **54**, 371–385 (1996).
12. J. T. Wang and I. S. Raju, Strain energy release rate formulae for skin-stiffener debond modeled with plate elements, *Engng. Fract. Mech*. **54**, 211–228 (1996).
13. O. Park, B. V. Sankar and R. T. Haftka, Buckling and postbuckling analysis of a stiffened panel with a skin-stiffener debond, in: *Proc. 13th Tech. Conf. Compos. Mater*., Baltimore, pp. 854–867 (1998).
14. H. Suemasu, M. Kasahara and T. Ishikawa, A numerical study on compressive behavior of blade stiffened plates with a debonding between a stiffener and a skin panel, *J. Japan Soc. Aeronaut. Space Sci.* **42**, 319–328 (1994).
15. H. Suemasu, K. Arai and T. Ishikawa, Compressive property of composite stiffened panel and debonding, in: *Proc. JSASS/JSME Struct. Conf.*, 173–175 (2002).
16. Habbitt, Karlsson and Sorensen, Inc., ABAQUS Theory Manual.